REJUVENATION RESEARCH
Volume 14, Number 1, 2011

DOI: 10.1089/rej.2010.1130

Therapeutic Efficacy of Intranasally Delivered Mesenchymal Stem Cells in a Rat Model of Parkinson Disease

Lusine Danielyan,[1] Richard Schäfer,[2,11] Andreas von Ameln-Mayerhofer,[3] Felix Bernhard,[1] Stephan Verleysdonk,[4,10] Marine Buadze,[1] Ali Lourhmati,[1] Tim Klopfer,[1] Felix Schaumann,[1] Barbara Schmid,[3] Christoph Koehle,[5] Barbara Proksch,[1] Robert Weissert,[6,13] Holger M. Reichardt,[7] Jens van den Brandt,[7] Gayane H. Buniatian,[1,12] Matthias Schwab,[1,8] Christoph H. Gleiter,[1] and William H. Frey II[9]

Abstract

Safe and effective cell delivery remains one of the main challenges in cell-based therapy of neurodegenerative disorders. Graft survival, sufficient enrichment of therapeutic cells in the brain, and avoidance of their distribution throughout the peripheral organs are greatly influenced by the method of delivery. Here we demonstrate for the first time noninvasive intranasal (IN) delivery of mesenchymal stem cells (MSCs) to the brains of unilaterally 6-hydroxydopamine (6-OHDA)–lesioned rats. IN application (INA) of MSCs resulted in the appearance of cells in the olfactory bulb, cortex, hippocampus, striatum, cerebellum, brainstem, and spinal cord. Out of 1×10^6 MSCs applied intranasally, 24% survived for at least 4.5 months in the brains of 6-OHDA rats as assessed by quantification of enhanced green fluorescent protein (EGFP) DNA. Quantification of proliferating cell nuclear antigen-positive EGFP-MSCs showed that 3% of applied MSCs were proliferative 4.5 months after application. INA of MSCs increased the tyrosine hydroxylase level in the lesioned ipsilateral striatum and substantia nigra, and completely eliminated the 6-OHDA–induced increase in terminal deoxynucleotidyl transferase (TdT)-mediated 2′-deoxyuridine, 5′-triphosphate (dUTP)-biotin nick end labeling (TUNEL) staining of these areas. INA of EGFP-labeled MSCs prevented any decrease in the dopamine level in the lesioned hemisphere, whereas the lesioned side of the control animals revealed significantly lower levels of dopamine 4.5 months after 6-OHDA treatment. Behavioral analyses revealed significant and substantial improvement of motor function of the Parkinsonian forepaw to up to 68% of the normal value 40–110 days after INA of 1×10^6 cells. MSC-INA decreased the concentrations of inflammatory cytokines—interleukin-1β (IL-1β), IL-2, -6, -12, tumor necrosis factor (TNF), interferon-γ (IFN-γ, and granulocyte-macrophage colony-stimulating factor (GM-CSF)—in the lesioned side to their levels in the intact hemisphere. IN administration provides a highly promising noninvasive alternative to the traumatic surgical procedure of transplantation and allows targeted delivery of cells to the brain with the option of chronic application.

[1]Department of Clinical Pharmacology, University Hospital of Tübingen, Tübingen, Germany.
[2]Institute of Clinical and Experimental Transfusion Medicine, University Hospital of Tübingen, Tübingen, Germany.
[3]Neuropharmacology, Institute of Neurobiology, University of Tübingen, Tübingen, Germany.
[4]Interfaculty Institute for Biochemistry, University of Tübingen, Tübingen, Germany.
[5]Department of Toxicology, Institute of Experimental and Clinical Pharmacology, University Hospital of Tübingen, Tübingen, Germany.
[6]Experimental Neuroimmunology Laboratory, Department of Neurology, University of Tübingen, Tübingen, Germany.
[7]Department of Cellular and Molecular Immunology, University of Göttingen Medical School, Göttingen, Germany.
[8]Dr Margarete Fischer-Bosch-Institute of Clinical Pharmacology, University of Tübingen, Stuttgart, Germany.
[9]Alzheimer's Research Center at Regions Hospital, HealthPartners Research Foundation, St. Paul, Minnesota.
[10]German University in Cairo, Al Tagamoa Al Khames, New Cairo City, Egypt.
[11]Harvard Stem Cell Institute, Department of Stem Cell and Regenerative Biology Harvard University, Cambridge Maasachusetts.
[12]Institute of Molecular Biology NAS RA, Yerevan, Armenia.
[13]Department of Neurology, University of Geneva, Geneva University Hospital, Geneva, Switzerland.

Introduction

Surgical transplantation of therapeutic cells into the brain is a commonly used method of cell application for cell-based therapy of neurodegenerative disorders. Its associated problems include graft rejection resulting from immunological response,[1,2] as well as the consequences of direct tissue trauma such as inflammation, cerebral edema, and reactive gliosis.[3–5] Insufficient graft survival after transplantation has been shown in a model of Parkinson disease (PD) and in the brains of normal rodents.[6–8]

Intravenous (i.v.) or intraarterial (i.a.) administration of cells is a less invasive delivery method compared to surgical transplantation. Despite the advantages of possible chronic application and absence of traumatic injury, both the i.v. and i.a. administration routes have significant side effects. i.v. administration results in either massive systemic distribution or entrapment of applied cells in peripheral organs such as lungs, liver, and spleen.[9,10] i.a. delivery of cells, e.g., to lesioned brain areas, is a more targeted approach,[11] but it may lead to microvascular occlusions, worsening the cerebral blood flow, which is often already compromised in neurodegenerative disorders such as stroke, Alzheimer disease, and PD.[12–14] Our previous work demonstrated in principle that intranasal (IN) application (INA) of mesenchymal stem cells (MSCs) results in the delivery of numerous stem cells to different brain areas of healthy rodents, including the olfactory bulb, cortex, and striatum.[15]

However, the long-term survival and therapeutic impact of stem cells administered by this route in experimental models of neurodegeneration has remained unexplored. Here we show the therapeutic effects of IN-delivered MSCs in the rat unilateral 6-hydroxydopamine (6-OHDA) lesion model of PD. Our data show that MSCs delivered to the lesioned striatum via INA survive for a period of at least 6 months and improve the previously depleted dopaminergic activity of the nigrostriatal system after unilateral 6-OHDA injection. In addition, IN-delivered MSCs show a strong antiinflammatory effect in the lesioned hemisphere and prominently improve the motor deficit.

Materials and Methods

Generation of enhanced green fluorescent protein transgenic dark agouti rats

Lentiviral particles were obtained by transfecting HEK293T cells with FUGW vector DNA and the helper plasmids pMDL-RRE, pRSV-REV, and pVSV-g, as described previously.[16] The virus was concentrated by ultracentrifugation, resuspended in phosphate-buffered saline (PBS), and titrated by serial dilutions on HeLa cells. Transgenesis was performed according to our established protocol[16] by injecting the lentiviral concentrate into the perivitelline space of fertilized single-cell embryos obtained from superovulated female Dark Agouti (DA/OlaHsd) rats (Harlan Winkelmann, Borchen, Germany). Two-cell stage embryos were transferred into the oviduct of pseudopregnant Crl:CD females (Charles River, Sulzfeld, Germany), and the offspring were analyzed for EGFP expression by flow cytometry. Due to the use of the ubiquitin-C promoter in the lentiviral vector, enhanced green fluorescent protein (EGFP) is expressed in essentially all cell types. All procedures were conducted according to Bavarian state regulations and approved by the responsible authorities (Regierung von Unterfranken).

Isolation and cultivation of bone marrow MSCs

EGFP-MSCs were isolated from the mononuclear cell fraction of pooled bone marrow (BM) from 10 EGFP-DA rats (females, age 1 month) after plastic adherence and were cultured (37°C, 5% humidified CO_2) with α-minimal essential medium (α-MEM; Cambrex Bio Science, Verviers, Belgium), containing desoxyribonucleotides (10 mg/L each, 11 mg/L 2′-deoxycytidine HCl), ribonucleotides (10 mg/L each), ultraglutamine (434 mg/L), 100 IU/mL penicillin (Cambrex Bio Science), 100 μg/mL streptomycin (Cambrex Bio Science), and 10% heat-inactivated (56°C, 30 min) fetal calf serum (FCS; Cambrex Bio Science). To determine the stem cell plasticity, trilineage *in vitro* differentiation was performed as described previously[17] and demonstrated by specific staining with Oil Red O (adipogenesis), alkaline phosphatase (osteogenesis), and safranin O (chondrogenesis). Fluorescence-activated cell sorting (FACS) analysis was performed with a FACScan instrument (BD Biosciences, San Jose, CA) using BD CellQuestPro software and the phycoerythrin (PE)-conjugated antibodies anti-rat-CD9, -CD11b/c, -CD29, -CD31, -CD34, -CD39, -CD44, -CD45, -CD73, -CD90, -CD106, -CD133, -CD143, -CD166, -CD200, -SSEA-1 (BD Biosciences; Santa Cruz Biotechnology, Santa Cruz, CA; Serotec, Raleigh, NC; Biolegend, San Diego, CA). The cells used in this study were positive for CD9, CD29, CD44, CD73, CD90, CD166, CD200, and SSEA-1 and negative for CD11b/c, CD31, CD34, CD39, CD45, CD106, CD133, and CD143.

Quantitative cell migration assay

To study the migratory potential of rat EGFP-MSCs, a two-compartment system was used where cells were induced to migrate from an upper compartment through a porous membrane into a lower compartment. EGFP-MSCs were seeded at a density of 4,000 cells/mm^2 in 75-cm^2 in cell culture flasks in Dulbecco modified Eagle medium (DMEM, high glucose; PAA, Coelbe, Germany) supplemented with 10% FCS, penicillin (100 U/ mL), and streptomycin (100 μg/ mL) and cultured in a humidified 10% CO_2 atmosphere at 37°C. After 72 h (≈75% confluence), cells were trypsinized, resuspended in supplemented DMEM, and seeded with a concentration of 8×10^4/200 μL onto a ThinCert™ cell culture insert (upper compartment, 8-μm pore size, translucent polyethylene terephthalate (PET) membranes, 24-well format, Greiner Bio One, Frickenhausen, Germany). Inserts (5 replicates) were placed into the wells of a 24-well plate (lower compartment), each containing 600 μL of control medium or the same medium supplemented with 100 ng/mL brain-derived neurotrophic factor (BDNF). The assembly was incubated for 4 h in a humidified 10% CO_2 atmosphere at 37°C. Thereafter, the inserts were removed, washed twice with phosphate-buffered saline (PBS), and transferred into the wells of a freshly prepared 24-well plate, each well containing 500 μL of 0.05% trypsin-EDTA solution (PAA). This plate was incubated for 10 min at 37°C in a hybridization shaker with an agitation of 70 strokes/min. Detached cells were counted in a Neubauer chamber for quantification of cells that actively migrated into the lower compartment. To determine the appropriate BDNF concentration, a pilot test with 12 ng/mL,

25 ng/mL, 50 ng/mL, and 100 ng/mL BDNF/mL of DMEM was performed. A concentration of 100 ng/mL of BDNF was found to be the most effective concentration to induce migration.

Animals

Male Sprague–Dawley rats (Charles River WIGA GmbH, Sulzheim, Germany), weighing 240–300 grams, were used for the IN delivery experiments. They were housed in groups of 3 or 4 animals in standard macrolon cages in a temperature- and climate-controlled room under a 12-h light/dark cycle (lights on at 7:00 a.m.) and had access to water (*ad libitum*) and standard food (15 grams per animal and day). All procedures were carried out in accordance with the ethical guidelines for use of animals in experiments and were approved by the administration office of the local governmental authority (Regierungspräsidium Tübingen).

Lesion surgery

For lesion of the dopaminergic neurons within the medial forebrain bundle (mfb), animals were deeply anesthetized with 64 mg/kg intraperitoneally (i.p) applied pentobarbital sodium (Narcoren®, Merial Hallbergmoos, Germany) or with isoflurane/fentanyl anesthesia. To ease breathing during anesthesia, each animal received a low-dose atropine sulfate injection (B. Braun, Melsungen, Germany, 0.5 mg/mL in 0.1 mL of saline). Thirty minutes before injection of the neurotoxin 6-OHDA, the animals received desipramine hydrochloride (Sigma Taufkirchen, Germany, 20 mg/kg, i.p.) to protect noradrenergic neurons against damage from 6-OHDA. Using a stereotactic frame (Stoelting, Wood Dale, IL) and microsyringes (1 μL, SGE syringes, Kiln Farm Milton Keynes, United Kingdom), 6-OHDA hydrobromide (12 μg free base diluted in 1 μL of 0.01% (wt/vol) ascorbic acid both Sigma) was infused into the left mfb at a rate of 1.0 μL/min using the following stereotaxic coordinates with respect to bregma: anterior–posterior (AP) = −4.0 mm, lateral (L) = +1.6 mm, and dosrsal–ventral (DV) = −8.8 mm from surface of the skull.[18] The injection cannula was left in place for additional 7 min to allow sufficient diffusion of 6-OHDA into the brain tissue. After surgery, the animals were single-housed for 1 day to allow for adequate recovery. To prevent animals from dehydrating, a commercial mineral solution (Jonosteril, Fresenius Kabi Deutschland GmbH, Bad Homburg, Germany; 3 mL/animal per day, i.p.) was additionally infused to animals for a maximum of 2 days postsurgery. Analgesic treatment was performed using carprofen (5 mg/kg; Rimadyl, Pfizer, Germany) immediately after surgery until 2 days postsurgery.

Cell application

IN cell or vehicle (PBS) application was performed during a short anesthesia (ketamine, 75–100 mg/kg, i.p.; Ketavet, Pfizer). Prior to vehicle or cell treatment, all animals received IN 100 U hyaluronidase (Sigma) dissolved in 24 μL of sterile PBS. Rats received twice for each nostril alternate applications (left–right) of 6-μL drops containing cell suspension/hyaluronidase or PBS (the second set of right–left applications was performed 2 min after the first set). One hour after IN pretreatment with hyaluronidase, MSC suspension (3×10^5 or 5×10^5 in 24 μL of sterile PBS) or vehicle (PBS) was applied following the same procedure, i.e., in alternating 6-μL portions for each nostril.

For quantification of radiolabeled MSCs, conventional or laser scanning (LSM) fluorescence microscopy of EGFP-MSCs, and immunohistochemical analyses of tyrosine hydroxylase (TH), proliferating cell nuclear antigen (PCNA)-, smooth muscle α-actin (SMAA), β-tubulin III, and assessment of behavioral tests during a period of 6.7 months (data not shown), 3×10^5 cells were applied IN on day 3 postsurgery. The therapeutic efficacy of INA of 1×10^6 EGFP-MSCs in a follow-up study was evaluated by EGFP DNA quantification, western blots, quantification of terminal deoxynucleotidyl transferase (TdT)-mediated 2′-deoxyuridine, 5′-triphosphate (dUTP)-biotin nick end labeling (TUNEL)-, visualization and counting of PCNA- or TH-positive cells, and multiplex measurement of cytokines. For this experimental set, the animals ($n \geq 10$) were treated with 5×10^5 cells (1×10^6 cell in total) on days 7 and 9 postsurgery and sacrificed 4.5 months later.

Radiolabeling of MSCs

For radiolabeling of rat MSCs with tritiated thymidine, cells were seeded at approximately 20% confluency into 75-cm^2 cell culture flasks (Nunc, Wiesbaden, Germany) and cultivated in the presence of 1 μM thymidine and 370 kBq [*methyl*-^{3}H] thymidine (TRK418, GE Healthcare, Munich, Germany) per mL of medium for 1 week. After three washing steps (PBS), the medium was replaced by one devoid of radiolabel, and the cells were cultivated for an additional week with daily medium renewals. The absence of diffusible radiolabel from the final medium supernatant prior to trypsinization was confirmed by liquid scintillation counting (LKB Rackbeta 1219, Wellesley, MA) in Ultima Gold™ (Perkin Elmer, Waltham, MA; 5 mL in 20-mL vials) for 10 min per sample. After detachment by trypsinization, an aliquot was used for the determination of the cell number in a Neubauer chamber, and the degree of label incorporation into the cellular DNA was measured in another aliquot by liquid scintillation counting. The radioactivity per labeled MSC was determined as the measured radioactivity of the cell lysate divided by the counted cell number.

The labeled cells were then applied intranasally to rats (3×10^5 cells per animal, $n = 6$). After 4 h, the animals were sacrificed under ketamine anaesthesia (100 mg/kg; Ketavet, Pfizer) and the organs (heart, kidneys, lung, stomach, liver, spleen, spinal cord, and brain) were removed, weighed, and sampled. The brain was immediately dissected on an ice-cooled block into olfactory bulb (OB), cortex, striatum, hippocampus (HC), cerebellum (Cer), and brainstem according to the method described by Heffner et al.[19] and Mayerhofer et al.[20] The remaining brain tissue was collected as the sample "remaining brain." All samples were minced with scissors and then completely homogenized in deionized water using a Potter-Elvehjem homogenizer at 4,000 rpm. The samples were transferred to scintillation vials, mixed with 2 volumes of Ultima Gold™ scintillation fluid, and assayed for radioactivity by liquid scintillation counting (measuring time, 10 min per sample). The number of MSCs per organ was calculated as the measured sample radioactivity multiplied by the ratio of organ and sample weight and divided by the determined radioactivity per labeled MSCs (0.074 Bq).

Quantitative real-time polymerase chain reaction

Genomic DNA was extracted from one cerebral hemisphere per rat of a total of six, as well as from cultured EGFP-transgenic rat MSCs via a standard protocol including proteinase K digestion and phenol–chloroform extraction. One hundred nanograms of genomic DNA was analyzed by real-time quantitative PCR in a LightCycler instrument, using the FastStart DNA Master SYBR Green I kit (Roche, Basel, Switzerland). MSC genomic DNA content was quantified by a PCR assay for EGFP. PCR was performed for 45 cycles that each consisted of denaturation at 95°C for 5 s, annealing at 70°C for 3 sec, and extension at 72°C for 8 sec, using 3 mM $MgCl_2$ and the following primer set: forward, 5′-GTCCAGG AGCGCACCATCTTC-3′ and reverse, 5′-GATGCCGTTCTT CTGCTTGTCG-3′. Total levels of genomic DNA were determined by a PCR assay targeting exon 5 of the EPO gene. The primers used were: Forward, 5′-GGCTTCCTGATGCC ATGTG-3′ and reverse, 5′-TGGTGATTTCGGCTGTTGC-3′. To determine copy numbers (genome equivalents) of genomic MSC DNA and total DNA present in brain samples, standard curves were generated by logarithmic dilutions (100–0.01 ng) of MSC genomic DNA. For conversion to genome equivalents, the rat haploid genome size was assumed to be 2.82×10^9, which is equivalent to 6.2 pg DNA per cell.

The EGFP DNA readings were converted to the numbers of cells by dividing the amount of EGFP DNA in each sample by the DNA content of a single MSC (6.2 pg). The total DNA content in the brain (including cerebral and cerebellar hemispheres, olfactory bulbs, and brainstem) was 1.28 ± 0.06 mg (mean ± standard error of the mean [SEM], $n = 6$), corresponding to a total of 2.06×10^8 cells.

Experimental design for stepping test

Baseline stepping data were obtained from each rat 4–6 days prior to 6-OHDA surgery. On the day of surgery (d0), 6-OHDA was microinfused into the left mfb as described above. Animals had previously been assigned pseudorandomly to two treatment groups. On day 7 (in the morning), the first postlesion stepping test was performed (baseline PD-symptomatic measurement). Thereafter (in the afternoon), the first IN cell application was carried out: animals in the cell-treated group ($n = 9$) received 5.0×10^5 cells IN, whereas control animals ($n = 7$) received vehicle (PBS). On day 9, the treatment was repeated (INA of additional 5.0×10^5 cells or vehicle). On days 11, 13, 15, 21, 40, 42, 75, 90, and 110, all animals were tested for stepping performance. Thereafter animals were sacrificed (under anesthesia), and the brains were removed and frozen on dry ice.

Experimental design for rotometer test

The same 6-OHDA surgery as described above was performed for this experimental set. On day 3 after surgery (d3), all animals were tested for rotational behavior after a subcutaneous (s.c.) injection of 2 mg/kg D-amphetamine (Sigma Deisenhofen, Germany). The sufficiently lesioned animals were identified and randomly assigned to "cell" ($n = 12$) and "control" ($n = 10$) treatment groups. MSC application was performed in the same way as described above (5.0×10^5 cells IN or vehicle on 2 separate days, 7 and 9). On days 17, 105, and 136, rotometer tests were performed as described below. Thereafter animals were sacrificed under anesthesia; their brains were removed and frozen on dry ice.

Behavioral testing

The behavioral tests (stepping and rotational behavior) were performed in separate groups of animals (9 animals in cell-treated vs. 7 control animals for stepping test and 12 cell-treated vs. 10 control rats for rotational behavior) as described below.

Stepping test

To assess the motor performance of each forepaw, all animals were subjected to the correction stepping test ("stepping test") on several days according to the procedure described by Olsson et al.[21] and Tillerson et al.[22] For this purpose, every animal was gently taken into both hands of the experimenter in a way that only one forepaw hung out of the grip in a relaxed state. The rat was gently and slowly moved sideways over a wooden bar (100 cm length, over 15 s). Each extremity was moved sideways in two directions (a push condition, left paw moved to the left, right paw moved to the right, and a pull condition, left paw to the right, right paw to the left). This procedure was repeated three times per test day with every rat. The stepping ratio was calculated by dividing the median stepping number of the ipsilateral paw by the median stepping number of the contralateral paw separately for every condition (push and pull). From these two results, a mean stepping ratio was calculated for every rat. The data presented in Fig. 7B, below, result from the formula: Mean stepping ratio = [(contralateral push/ipsilateral push) + (contralateral pull/ipsilateral pull)]/2.

Rotational behavior

On days 3, 17, 105, and 136 postsurgery, the rotational behavior was measured in a rotometer system (TSE, Technical & Scientific Equipment GmbH, Bad Homburg, Germany). One 360° turn was counted as a rotation; the activity of the animals was recorded every 10 min. The "net ipsilateral rotations" number was calculated as the difference of ipsilateral − contralateral rotations within a 100-min timeframe (30–120 min after the injection of 2 mg/kg D-amphetamine, corresponding to the time from maximal increase of rotation (according to Ungerstedt and Arbuthnott[33]) to the end of observation period). A significant increase in rotations over time as observed in our study is not unusual and is most likely based on a behavioral sensitization process known for psychostimulants (e.g., amphetamine) or dopamine deficiency states or combinations of both.[23–26]

Preparation of brain sections

Horizontal cryosections (20 μm in thickness) were prepared from the whole brains of rats. For detection of EGFP-MSCs by fluorescence and confocal LSM, the sections were stained with 4′,6 diamidino-2-phenylindole (DAPI; Vector Laboratories Burlingame, CA). For quantification of EGFP-MSCs, horizontal sections from the area between −2 mm and −8 mm from the surface of the brain were analyzed by fluorescence microscopy using an Olympus BX51 microscope (Olympus, Hamburg, Germany) and AnalySIS software (Soft Imaging System GmbH, Germany). For LSM, the selected sections

containing EGFP-MSCs were analyzed by the Fluoview FV10i system (Olympus) equipped with four (405/473/559/625 nm) diode lasers. The numbers of EGFP-positive MSCs in different areas of the brain were obtained by extrapolating from the total number of screened sections (300 sections/brain) to the volume of 1 mm^3.

TH, β-tubulin III, PCNA, and SMAA staining

Horizontal sections of 6-OHDA-lesioned rat brains, selected from the neighborhood of the sections containing EGFP-MSCs, were fixed with methanol at −20°C, washed, and subsequently incubated with monoclonal antibodies against TH diluted 1:100 (Chemicon, Schwalbach, Germany), or SMAA diluted 1:30 (Progen, Heidelberg, Germany), or PCNA diluted 1:25 (Chemicon), or β-tubulin III clone TUJ1 diluted 1:250 (R&D Systems, Wiesbaden-Nordenstadt, Germany) for 2 h at room temperature. Sections treated with PCNA, TH, or SMAA antibodies were washed with PBS and further incubated with Cy3-conjugated goat anti-mouse immunoglobulin G (IgG) diluted 1:500 (Dianova, Hamburg, Germany) for 1 h at room temperature. Thereafter, samples were washed with 0.1% Triton (Sigma) in PBS, coated with Vectashield mounting medium containing DAPI (Vector Laboratories Burlingame, CA), and assessed by fluorescence microscopy.

The number of TH-positive cells in the substantia nigra (SN) was determined from brain slices displaying a cross section of the entire SN. Every second section throughout the entire SN and the striatum (for the quantification of TH + area), respectively, was analyzed, the total numbers being 15 for the SN and 25 for the striatum per animal. The total number of TH-positive cells in SN from screened sections was extrapolated to 1 mm^2.

TUNEL staining

For quantification of TUNEL-positive host cells in striatum and SN, selected brain sections ($n = 10$) from four brains of each cell- and vehicle-treated group were washed with PBS, stained via the TMRred In Situ Cell Death Detection kit according to the protocol of the manufacturer (Roche Diagnostics, Mannheim, Germany) and mounted with Vectashield mounting medium containing DAPI.

Western blot analyses

Western blotting was performed using protein lysates from individual brain hemispheres. Protein concentrations were measured by the method of Bradford.[27] For each lane, 100 μg of protein was subjected to sodium dodecyl sulfate polyacrylamide gel electrophoresis (SDS-PAGE) in a 12.5% gel and transferred to polyvinylidene fluoride (PVDF) membranes by tank blotting. Membranes were blocked in 0.66% (vol/wt) I-Block (Tropix, Applied Biosystems, Weiterstadt, Germany) in PBS–Tween-20 (PBST; 0.05% Tween 20 in PBS, and pH 7.4) for 1.5 h and were then incubated at 4°C overnight with antibodies against tyrosine hydroxylase (1:1,000, Chemicon International, Nürnberg, Germany), BDNF (1:100, Millipore, Billerica, MA), leukemia inhibitory factor (LIF; 1:200, Santa Cruz Biotechnology, Santa Cruz, CA), and glyceraldehyde 3-phosphate dehydrogenase (GAPDH; 1:1,000, loading control, Chemicon International; Nürnberg, Germany). For visualization of antibody binding, membranes were incubated for 2 h at room temperature with alkaline phosphatase–conjugated goat anti-rabbit or mouse (Tropix) or donkey anti-goat secondary antibodies (Santa Cruz Biotechnology), diluted 1:10.000 in I- Block, and thereafter exposed to CDP-Star (Tropix) as a chemoluminescence substrate for 1 h in the dark room. Signal intensities were recorded using a CCD camera system, and subsaturated images were analyzed semiquantitatively by densitometry using the TINA software (version 2.09g, Raytest, Straubenhardt, Germany). Data were normalized to the respective densitometric values of normoxic controls and expressed as percent values.

Determination of cytokines in rat brain homogenate

Brains were removed, immediately frozen, and stored at −80°C until analysis. The brains were divided along the interhemispheric fissure; left and right hemispheres were weighed and analyzed separately. Ice-cold lysis buffer (300 mM NaCl, 50 mM Tris, 2 mM $MgCl_2$, 0.5% Nonidet P-40) containing a Complete Protease Inhibitor Tablet (Roche Diagnostics) was added at a ratio of 1/3 (weight/volume). The tissue was disrupted on ice by 15 strokes in a glass–glass homogenizer revolving at 1,200 rpm. Thereafter, homogenates were clarified by centrifugation for 10 min at 1,500 × *g*, and the supernatant was divided into aliquots and frozen at −80°C. Quantification of protein content was done by using the Bio-Rad DC Protein Assay (Munich, Germany) according to the manufacturer's manual. Determination of rat cytokines (interleukin-1α [IL-1α], IL-1β, IL-2, -4, -6, -10, -12, tumor necrosis factor-α [TNF-α], interferon-γ [IFN-γ], and granulocyte-macrophage colony-stimulating factor [GM-CSF]) was performed as described elsewhere.[28] Results were expressed in μg/g protein.

Statistical analyses

Statistical analyses of EGFP-MSCs, [^{3}H-Thy]-MSCs, TUNEL, TH, and cytokine quantifications were performed by the Student *t*-test for single comparisons and one-way analysis of variance (ANOVA) with Bonferroni test for multiple comparisons; $p < 0.05$ was considered as significant. The data are presented as mean ± SEM.

Results of the behavioral tests were analyzed by one-way (rotometer tests, each day separately) or two-way ANOVA (stepping test) with the factors "treatment" (between groups) and "time" (within subjects) followed by a post hoc Fisher least significant difference (LSD) test. The statistical results are provided in Tables 1 and 2.

Results

The efficacy of IN delivery of [^{3}H]thymidine-labeled MSCs ([^{3}H]Thy-MSCs) to the brain in unilaterally 6-OHDA–lesioned rats was evaluated by measuring the radioactivity in homogenates of various organs 4 h after INA. Among all analyzed organs, the highest amount of [^{3}H]Thy-MSCs appeared in the brain (Fig. 1A). Outside the central nervous system (CNS), the number of cells in the stomach was greater than that in all other peripheral organs, indicating that a considerable amount of MSCs was swallowed during INA. The distribution of [^{3}H]Thy-MSCs in the CNS revealed that in the 6-OHDA–lesioned brain, the highest percentage of

Table 1. Statistical Results of Data Analysis of Rotometer Tests by Means of a One-Way Analysis of Variance on Each Test Day Separately

Test day	*F(1,20)*	*p*
d3	<0.01	0.95
d17	1.19	0.29
d105	1.02	0.32
d136	4.46	0.048

cells appeared in cortex, cerebellum, brainstem, and spinal cord 4 h after application (Fig. 1B).

In the second part of our IN delivery efficacy study, we tested the survival of MSCs expressing EGFP in the brain over a time period of 4.5–6.7 months and their capacity to migrate to the 6-OHDA–lesioned striatum. The lesions of the ipsilateral (left) striatum and SN are reflected by the difference in their TH levels as compared to their intact contralateral counterparts both 7 days (cf. Fig. 2A vs. 2B) and 4.5 months (cf. Fig. 2C and 2D vs. 2F) after 6-OHDA injection into the left mfb. In the area of the lesioned striatum and the SN, the expression of TH was markedly increased by cell application (striatum in Fig. 2E and SN in Fig. 2G) in comparison to the control group (striatum in Fig. 2F and SN Fig. 2H) as measured 4.5 months after the experiment. This effect on TH expression appeared to be more prominent in the SN (cf. Fig. 2G vs. 2H) than in the striatum (cf. Fig. 2E vs. 2F).

Measurement of EGFP-MSCs in the brains 4.5–6.7 months after surgery and INA of either 1×10^6 or 3×10^5 cells was performed in two experimental sets by quantification of EGFP DNA and fluorescence microscopy, respectively. To evaluate the total number of MSCs delivered to the brain, we used quantified EGFP DNA. Quantification of MSCs by DNA analysis of EGFP showed that the mean total number of EGFP cells was $24.8\pm8\times10^4$ per brain ($n=5$). Thorough analysis of specific brain areas by fluorescence microscopy of EGFP-MSCs in the brain sections demonstrated significantly higher numbers of EGFP-MSCs in the ipsilateral striatum, lateral ventricles, and hippocampus as compared to the respective areas on the contralateral side (cf. HC ipsi vs. HC contra, LV ipsi vs. LV contra, striatum ipsi vs. striatum contra and SN ipsi vs. SN contra) after INA of 3×10^5 (Fig. 1C) or 1×10^6 cells (Fig. 1D). Out of all analyzed cerebral areas, the highest amount of EGFP-MSCs was observed in the lesioned striatum (Fig. 1C,D, striatum ipsi) followed by the SN (SN ipsi in Fig. 1D).

Some of the EGFP-MSCs detected in the lesioned striatum 6.7 months after INA of 3×10^5 MSCs bore processes (arrows in Fig. 3A). The quantification of these process-bearing EGFP-MSCs in different brain areas 4.5 months after application of 1×10^6 cells showed the highest amount of cells in the lesioned area, i.e., ipsilateral SN and striatum, as compared to the amount of cells in the respective contralateral SN and striatum (Fig. 4B) or the other brain areas on the ipsilateral side (Fig. 4C). Many of the detected cells (arrow in Fig. 3B) were adjacent to thread-like structures (arrowheads in Fig. 3B) identifiable either as β-tubulin III–positive nerve fibers (arrowhead in Fig. 3C) or as SMAA-positive blood vessels (arrowhead in Fig. 3D). In the lesioned striatum, a high number of EGFP-MSCs expressed TH (yellow cell in Fig. 3E) and PCNA (arrow in Fig. 3F). The quantification of TH-positive EGFP-MSCs (EGFP+TH+) revealed a significantly higher number of them in the lesioned (ipsilateral) SN than in the contralateral intact side (cf. EGFP+TH+ in ipsilateral SN vs. EGFP+TH+ in contralateral SN in Fig. 4A). Moreover, the population of EGFP+TH+MSCs prevailed over the population of EGFP+ TH- MSCs in the ipsilateral SN, whereas the number of cells in both populations was nearly equal in the contralateral SN (Fig. 4A). The comparison of the EGFP+PCNA+ cell populations in the ipsi- and contralateral hemispheres yielded a significantly higher amount of EGFP+/PCNA+ cells in the ipsilateral striatum, SN, and hippocampus (Fig. 4D). In total, 3.2% of the applied MSCs were proliferative 4.5 months after application. However, no tumor formation was observed throughout the entire sections analyzed from each animal. The influence of INA of MSCs on the dopaminergic activity of the host tissue is reflected by an increased expression of TH in the lesioned striatum and SN compared to the control. The number of TH-positive cells and the TH-positive area in the ipsilateral SN and ipsilateral striatum was significantly elevated 4.5 months after INA of MSCs (Fig. 4E,F). These data were confirmed by western blot analysis: TH expression in the ipsilateral side of the cell-treated group was higher than that in the ipsilateral side of control brains (Fig. 5A, cf. ipsi cell vs. ipsi control).

Because BDNF facilitates differentiation of MSCs into functional neurons,[29] we tested the expression levels of BDNF in ipsi- and contralateral brain hemispheres. In both control and cell-treated groups, the levels of BDNF were higher in the ipsilateral side (Fig. 5A). Assuming that targeted migration of MSCs to the lesioned area could be at least partially due to the increase in BDNF in the 6-OHDA–injured hemisphere, we tested the influence of BDNF on the migration of MSC *in vitro* using a migration assay shown schematically in Fig. 5C. Indeed, the number of MSCs that reached the bottom side of the membrane (red cells in Fig. 5C) was markedly increased by the presence of 100 ng/mL BDNF in the cell culture medium (Fig. 5D). LIF is proposed to play a role in the initiation of chemotaxis and migration of MSCs.[30] Downregulation of LIF in the lesioned side (Fig. 5A) in both cell-treated and control groups suggests that, at least in this particular model of PD, this factor is not involved in lesion-targeted migration of MSC. Quantification of TUNEL-positive cells in striatum and SN clearly reveals the strong capacity of MSC to decrease the apoptosis of the host cells in these brain areas (Fig. 5B). Assessment of dopamine levels in the brain homogenates provided a further indication of the therapeutic influence of INA of MSCs. The levels of dopamine in the ipsi- and contralateral hemispheres of the cell-treated group were nearly equal, whereas a dramatic difference was observed between the ipsi- and contralateral hemispheres of the control group (Fig. 5E).

Table 2. Statistical Results of Data Analysis of Stepping Tests by Means of Repeated Measures Two-Way Analysis of Variance over Days 7–110

Factor	*F*	*df*	p
Treatment	47.97	1, 14	<0.0001
Time	20.75	8, 112	<0.0001
Treatment×time	16.11	8, 112	<0.0001

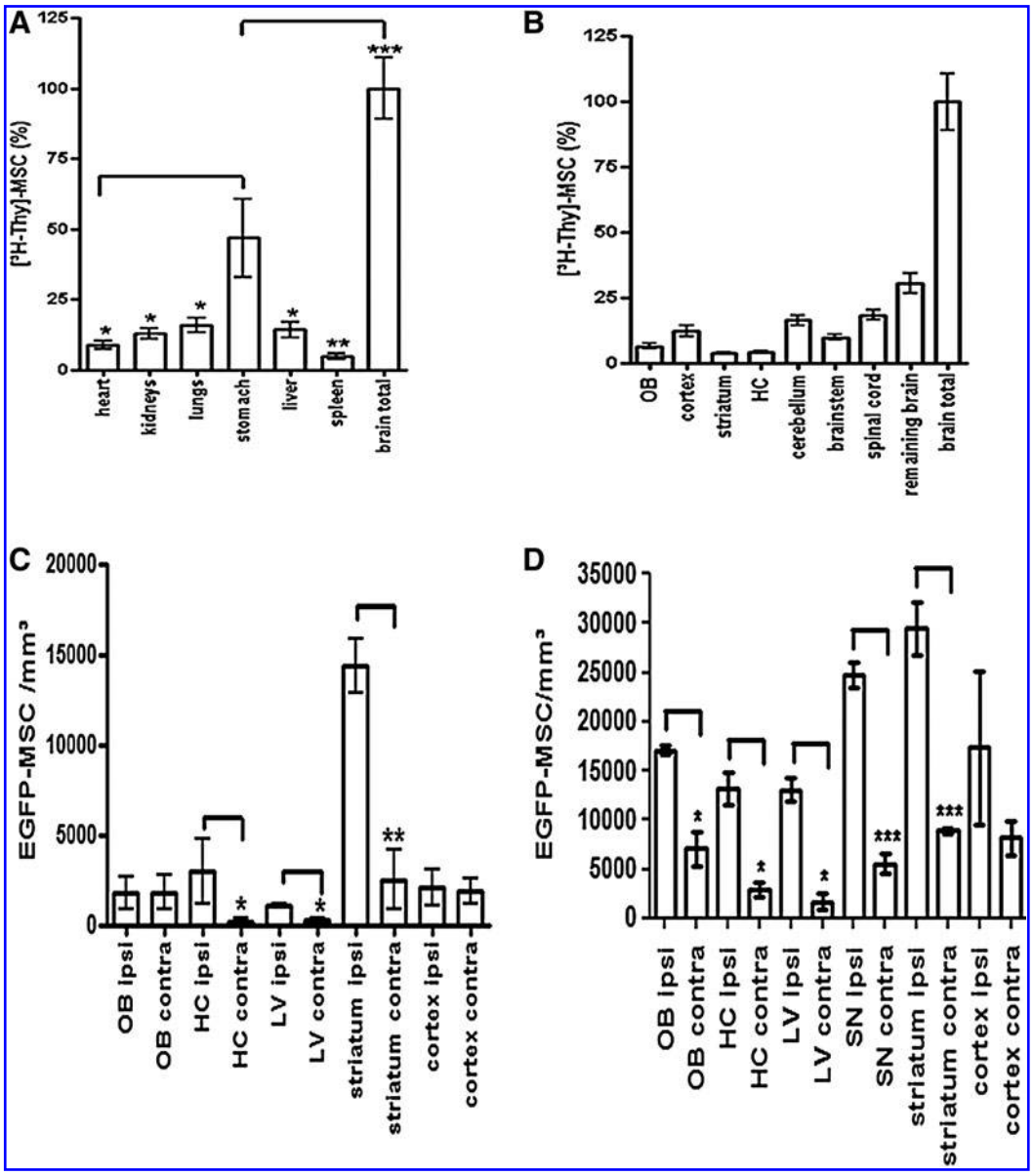

FIG. 1. Quantification of mesenchymal stem cells (MSCs) in the central nervous system (CNS) and other organs after intranasal application (INA). (**A**) Detection of [^{3}H]thymidine-labeled MSCs ([^{3}H]Thy-MSCs) in the brain, spinal cord, and other organs 4 h after INA of 3×10^5 cells to 6-hydroxydopamine (6-OHDA)–lesioned rats. (**B**) Detection of [^{3}H]Thy-MSCs in the left and right olfactory bulb (OB), cortex, striatum, hippocampus (HC), cerebellum, brainstem, spinal cord, and the remaining brain. The data in **A** and **B** are shown as percentage of the total amount of cells detected in the brain (brain total, $n=6$); **C** and **D** Quantification of enhanced green fluorescent protein (EGFP)-MSCs by fluorescence microscopy in ipsi- and contralateral olfactory bulb (OB), hippocampus (HC), lateral ventricle (LV), SN, striatum, and cortex brain of 6-OHDA–lesioned animals ($n=4$) 6.7 months after lesion and application of 3×10^5 EGFP-MSCs (**C**) or 4.5 months after lesion and application of 1×10^6 EGFP-MSCs. Data are presented as mean ± standard error of the mean (SEM). ($p<0.05$ one-way analysis of variance [ANOVA]).

The higher level of dopamine in the control contralateral hemisphere in comparison to the cell-treated contralateral side is related to the lesion-induced dopaminergic overcompensation in the intact nigrostriatal system, as reflected by increase in the stepping performance of the ipsilateral forepaw of unilaterally lesioned animals compared to the sham-lesioned animals.[21,31] The level of dopamine in the ipsilateral hemisphere of the cell-treated group was higher than that of the ipsilateral hemisphere of the control group (cf. ipsi in cell and control group in Fig. 5E).

Regarding the contribution of neuroinflammation to neuronal degeneration in PD widely discussed in the literature (for review, see ref. 32), we compared the levels of inflammatory cytokines in intact and lesioned hemispheres of both cell-treated and control groups. Figure 6 shows dramatically higher levels of IL-1β, IL-2, 6, 12, TNF-α, IFN-γ, and GM-CSF in the lesioned brain halves (BH) of control groups 4.5 months after the 6-OHDA-lesion (Fig. 6). INA of MSC (1×10^6 cells) decreased the levels of proinflammatory cytokines in the lesioned BH (Fig. 6). While differences in the levels of

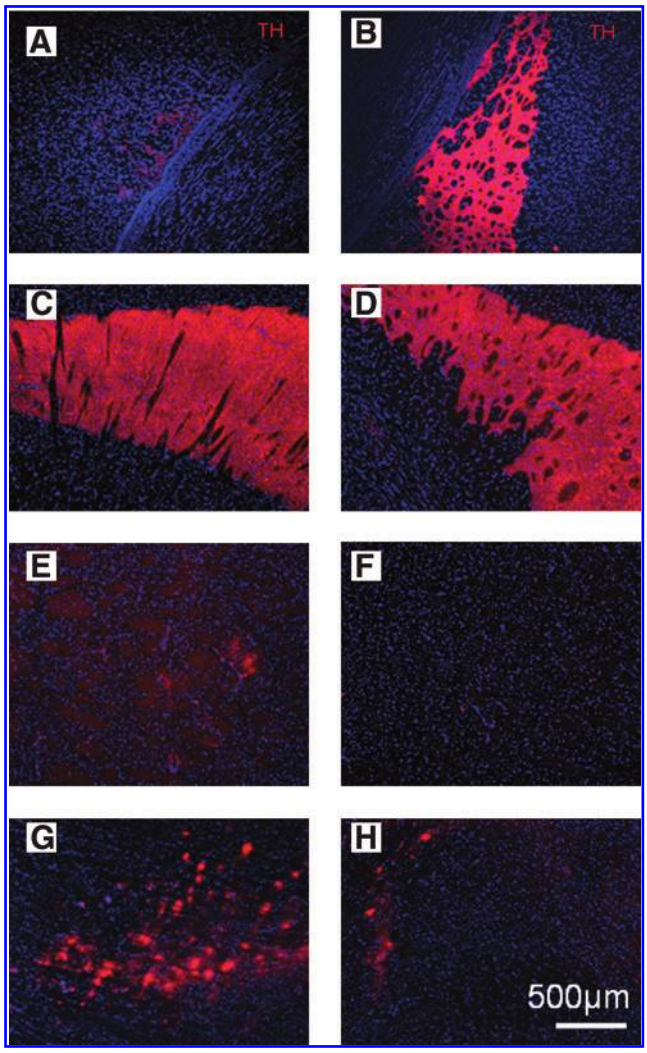

FIG. 2. Expression of tyrosine hydroxylase (TH) (red fluorescence) in the ipsilateral, lesioned and contralateral, intact striatum or substantia nigra (SN), respectively, of 6-hydroxydopamine (6-OHDA)–injected rats 7 days (**A,B**) or 4.5 months (**C–H**) after INA of 3×10^5 (**A,B**) or 1×10^6 enhanced green fluorescent protein mesenchymal stem cells (EGFP-MSCs) (**C–H**). (**A**) Ipsilateral, lesioned striatum 7 days after lesion of cell-treated animal. (**B**) Contralateral, intact stritatum 7 days after lesion of cell-treated animal. (**C**) Contralateral, intact striatum of cell-treated animal. (**D**) Contralateral, intact striatum of the control animal. (**E**) Ipsilateral, lesioned striatum of cell-treated animal. (**F**) Ipsilateral, lesioned striatum of the control animal. (**G**) Ipsilateral SN of cell-treated animal. (**H**) Ipsilateral SN of control animal. The cell nuclei are stained with 4′,6 diamidino-2-phenylindole (DAPI) (blue). Scale bar in **A–H**, 500 μm.

IL-1α (Fig. 6A) and IL-10 (Fig. 6C) were noticeable but not statistically significant, other inflammatory cytokines, IL-1β, IL-2, 6, 12, TNF, IFN-γ, and GM-CSF, were significantly lower in the ipsilateral BH of MSC-treated as compared to control animals (Fig. 6B,D–I). Out of the 10 analyzed cytokines, only IL-4 was undetectable (not shown).

Furthermore we tested the effect of IN application of EGFP-MSCs on the behavioral motor performance of unilaterally 6-OHDA–lesioned animals. Application of 3×10^5 EGFP-MSCs did not lead to significant changes in motor performance, as assessed by stepping ratio and amphetamine-induced rotations during 6.7 months after cell application (data not shown). Therefore, in our next experimental set we used INA of 1×10^6 cells divided into two equal applications on day 7 and day 9 (Fig. 7A,B).

MSC-treated ($n=9$) and vehicle-treated ($n=7$) groups did not differ in behavioral tests before cell treatment, i.e., day 7 (Fig. 7A), or day 3, respectively (Fig. 7B). Decreased rotational behavior in MSC-treated animals occurred on day 136 after surgery (Fig. 7B). Amphetamine-induced rotational behavior quantification is a well-established method for assessment of the nigrostriatal dopaminergic dysbalance in unilaterally 6-OHDA–lesioned rats.[33] Decreased rotations of the cell-treated group indicate behavioral compensation due to therapeutic effects of the INA of MSCs. Stepping ratios were initially increased in both treatment groups (Fig. 7A, days 9–42). Thereafter, both groups demonstrated a diver-

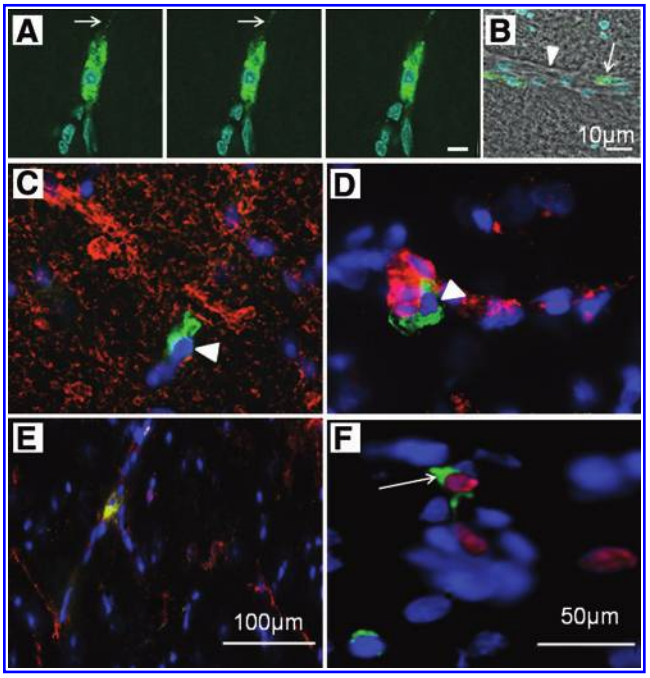

FIG. 3. Brain sections of 6-hydroxydopamine (6-OHDA) rats 6.7 months after application of 3×10^5 enhanced green fluorescent protein mesenchymal stem cells (EGFP-MSCs) (**A–D**) and 4.5 months after application of 1×10^6 EGFP-MSCs (**E,F**). (**A**) Z-stacks of EGFP-MSCs (green) obtained by laser scanning microscopy (3-μm steps) of sections from the ipsilateral striatum. Nuclei are stained with 4′,6 diamidino-2-phenylindole (DAPI)(blue). (**B**) Localization of EGFP-MSCa (green) adjacent to thread-like structures. (**C**) Localization of EGFP-MSCs (green) at nerve fibers stained with antibodies against tubulin beta III (red). (**D**) Localization of EGFP-MSCs adjacent to a smooth muscle α-actin (SMAA)-positive capillary (red). (**E**) Tyrosine hydroxylase (TH) (red)- and EGFP (green)-positive MSCs (yellow cell) in the ipsilateral striatum. (**F**) MSCs showing proliferating cell nuclear antigen (PCNA) signal (red), as well as 4′,6 diamidino-2-phenylindole (DAPI) (blue) and EGFP (green) fluorescence in the ipsilateral striatum. Scale bars: **A** and **B,** 10 μm; **C,D,F,** 50 μm; **E**,100 μm.

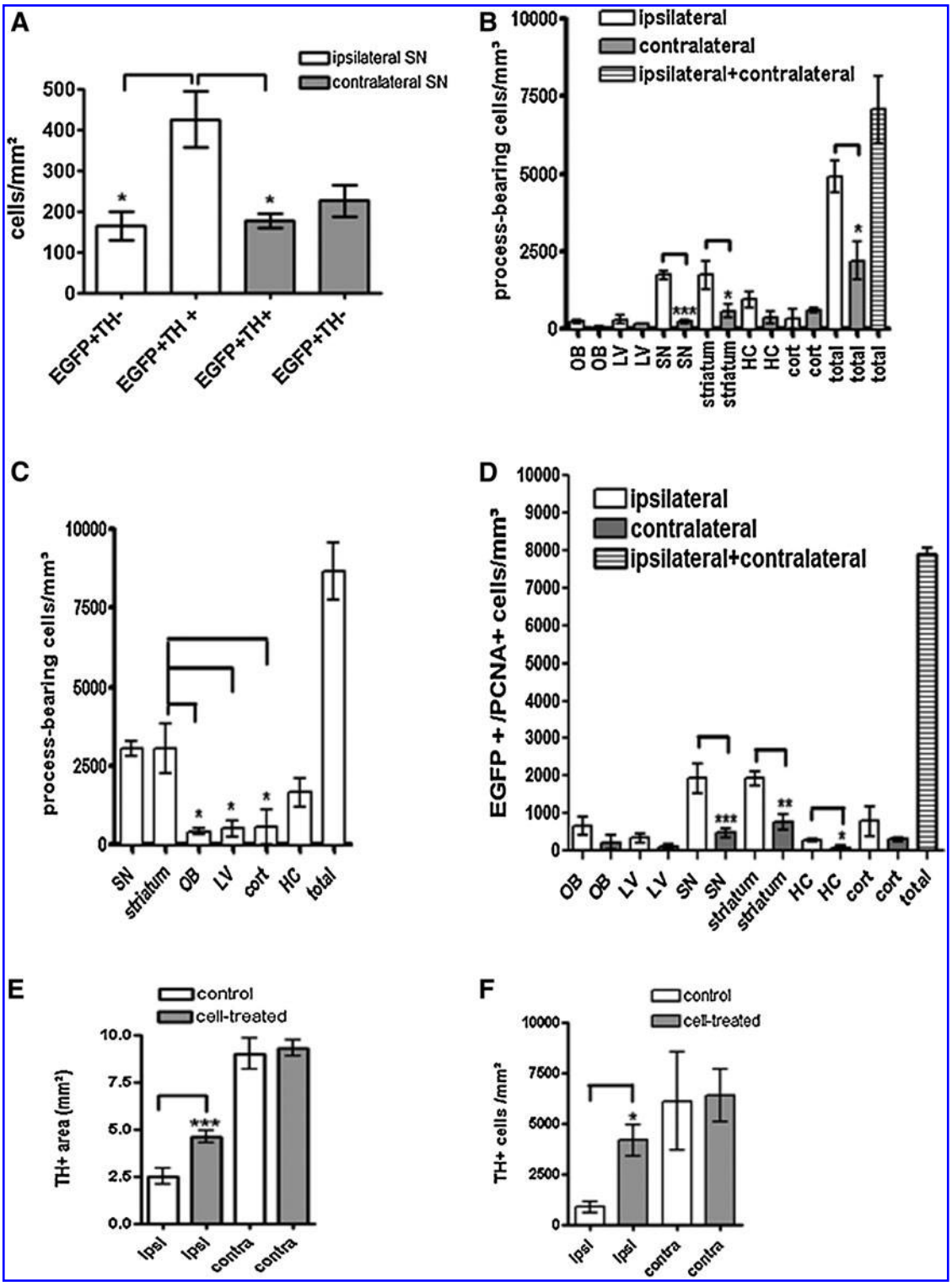

FIG. 4. Quantification of process-bearing or proliferating mesenchymal stem cells (MSCs) and expression of tyrosine hydroxylase (TH) in MSCs and in the host tissue of 6-hydroxydopamine (6-OHDA)–lesioned rats 4.5 months after intranasal application (INA) of 1×10^6 enhanced green fluorescent protein mesenchymal stem cells (EGFP-MSCs). (**A**) Quantification of EGFP+/TH− and EGFP+/TH+ populations of MSCs in the ipsi- and contralateral substantia nigra (SN). (**B,C**) Quantification of process-bearing MSCs in the ipsi- (**B,C**) and contralateral (**B**) olfactory bulb (OB), lateral ventricle (LV), SN, striatum, hippocampus (HC), and cortex. (**D**) Proliferating cell nuclear antigen (PCNA)-positive EGFP-MSCs in different ipsi- and contralateral brain areas. (**E**) Area of TH-positive host tissue in the ipsi- and contralateral striatum of MSC-treated animals. (**D**) Quantification of TH-positive cells in the SN of MSC-treated animals. Data in **A–F** are presented as mean ± standard error of the mean (SEM) ($p < 0.05$ one-way analysis of variance [ANOVA]).

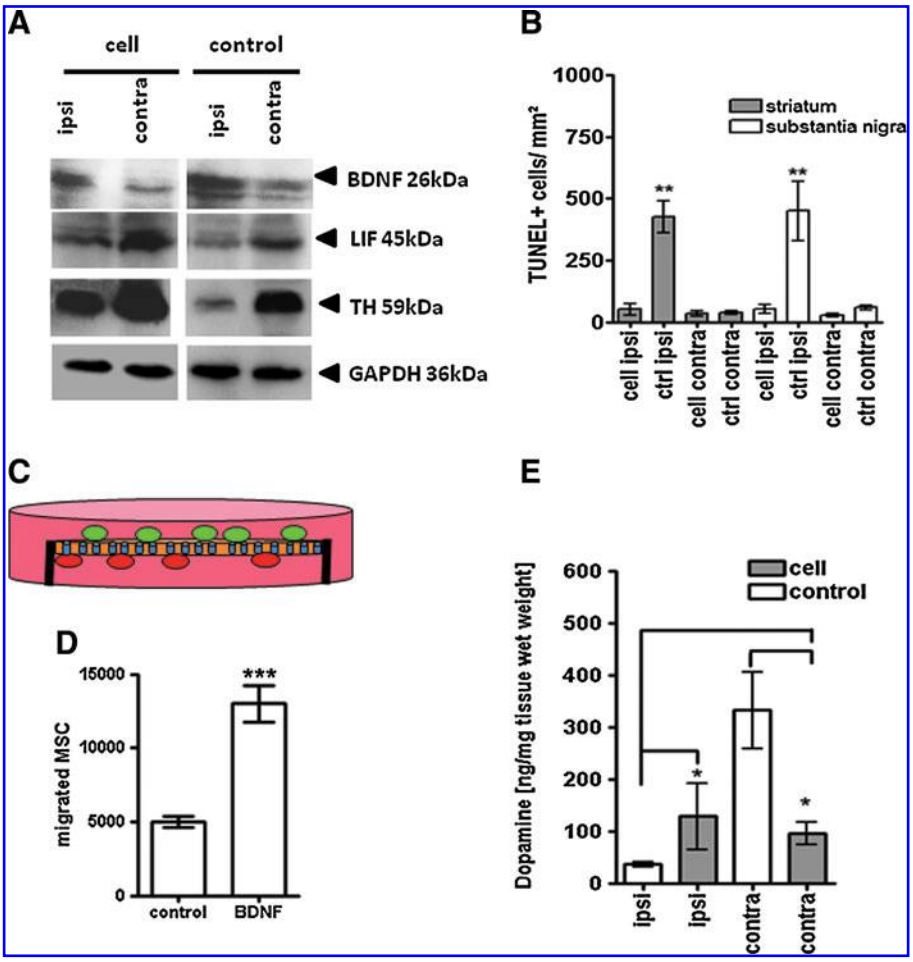

FIG. 5. (**A**) Western blot analyses of brain-derived neurotrophic factor (BDNF), leukemia inhibitory factor (LIF), and trysoine hydroxylase (TH) in the ipsi- and contralateral hemispheres; glyceraldehyde 3-phosphate dehydrogenase (GAPDH) serves as a loading control. (**B**) Terminal deoxynucleotidyl transferase (TdT)-mediated 2′-deoxyuridine, 5′-triphosphate (dUTP)-biotin nick end labeling (TUNEL)-based quantification of apoptosis in ipsi- and contralateral striatum and substantia nigra 4.5 months after application of 1×10^6 enhanced green fluorescent protein mesenchymal stem cells (EGFP-MSCs) ($n=4$). Data are presented as mean ± standard error of the mean (SEM). ($p<0.05$, one-way analysis of variance [ANOVA]). (**C**) Schematic drawing of the *in vitro* migration MSC assay; cells migrate from the compartment above the membrane (pore size, 8 μm; green cells) to the bottom side (red cells). (**D**) Quantification of the MSCs migrated toward the control and the BDNF-supplemented culture medium. (**E**) Dopamine content of the ipsi- and contralateral hemispheres of the cell- and vehicle-treated animals 4.5 months after application of 1×10^6 MSCs. Data are presented as mean ± SEM ($p<0.05$ one-way ANOVA).

gent behavior over time: while stepping ratios of the control animals decreased from day 75 to 110, cell treated animals remained on the higher stepping ratio level (Fig. 7B).

Discussion

This study demonstrates for the first time the therapeutic efficacy of IN-delivered MSCs to the brain in an animal model of PD. Successful delivery of INA MSCs to the unilaterally 6-OHDA–lesioned brain was demonstrated at 4 h, 4.5 months, and 6.7 months after INA of MSCs.

The distribution of [^{3}H]Thy-MSCs in the CNS revealed that, unlike our previous data showing the highest amount of cells in the olfactory bulb 1 h after application in healthy rodents,[15] in the 6-OHDA–lesioned brain the highest percentage of cells was observed in cortex, cerebellum, brainstem, and spinal cord 4 h after INA. These findings provide further evidence for our previously suggested migrational routes of INA cells into the brain along the olfactory and trigeminal nerves via parenchymal and CSF pathways.[15] These delivery routes are also known to be involved in the rapid IN delivery of drugs to the brain.[34,35] On the basis of our observation that a large portion of the INA MSCs rapidly reached the brainstem and spinal cord, as assessed by quantification of radiolabeled cells 4 h after INA, IN delivery may be an especially useful method of therapeutic cell administration for diseases associated with brainstem and spinal cord pathology, such as brain stem infarction, traumatic injuries, amyotrophic lateral sclerosis (ALS), and multiple sclerosis.

INA of MSCs results in their long-term survival and exhibition of dopaminergic features reflected by their expression of TH. A small portion of delivered MSCs (3.2% out of 24.8×10^4 cells) expressed PCNA, possibly reflecting the renewal of the MSC population in the host tissue. This popu-

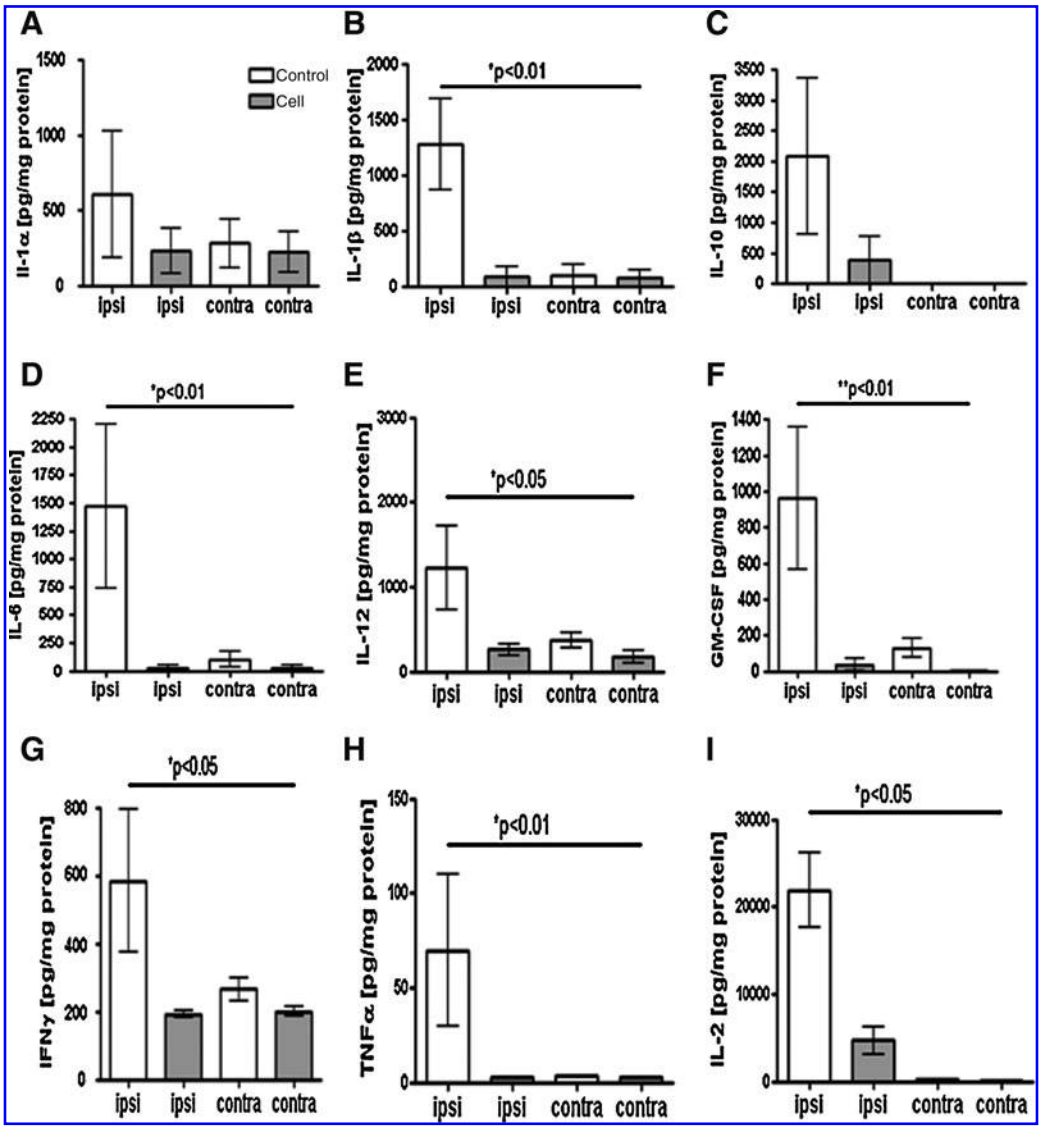

FIG. 6. Quantification of interleukins (IL) in the ipsilateral (ipsi) and contralateral (contra) hemispheres in the brains of 6-hydroxydopamine (6-OHDA)–lesioned rats 4.5 months after intranasal application (INA) of phosphate-buffered saline (PBS) (control, grey bars) or 1×10^6 of enhanced green fluorescent protein mesenchymal stem cells (EGFP-MSCs) (cell, white bars). The data were statistically compared by one-way analysis of variance (ANOVA) with the Dunett *post hoc* test and are shown as mean ± standard error of the mean (SEM) ($n = 5$, $p < 0.05$).

lation was located predominantly in the lesioned area (ispilateral striatum and SN), indicating that the proliferative activity of MSCs, restricted to the areas alongside the degenerated regions, would minimize their long-term persistence in remaining brain areas and thus their influence on intact host tissues. INA of MSCs led to therapeutic effects on dopaminergic activity, reflected by increases in TH and dopamine levels in the lesioned areas (striatum and SN) of the host tissue. This effect may result from: (1) Replacement of degenerated striatal and nigral tissue by TH-positive MSCs; and/or (2) neuroprotective effects of the MSCs on the brain due to trophic and antiinflammatory activities of the MSCs. However, because the effects of MSCs on the number of TUNEL-positive host cells and the levels of inflammatory cytokines were more prominent than the ability of MSCs to eliminate the dysbalance in TH and dopamine between ipsi- and contralateral sides, it is likely that the neuroprotective features of MSC may prevail over their capacity to replace degenerated neural cells.

Another question addressed here is whether INA of MSCs would lead to the targeted delivery of cells to the lesioned area, and whether this process may involve a local increase in certain factors affecting the migration of MSCs. Indeed, the level of BDNF, but not that of LIF, was clearly increased in the ipsilateral hemisphere compared to the contralateral side, and BDNF appeared to serve as a migration-stimulating factor for MSCs, as shown by our *in vitro* experiments. Recent studies have shown that the increase in BDNF levels in the brain is not only relevant to PD[36,37] but also to Alzheimer disease (AD) pathology. The serum levels of BDNF are increased in patients with AD or mild cognitive impairment[38] and amyloid beta (Abeta) 1–42 appears to increase the

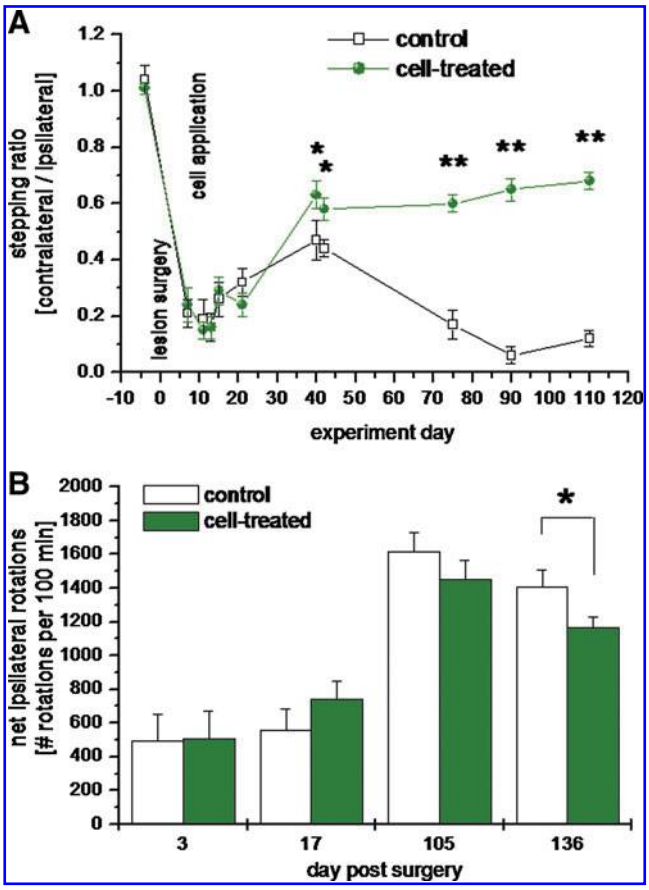

FIG. 7. Analysis of the behavior in 6-hydroxydopamine (6-OHDA)–lesioned rats 4.5 months after delivery of 1×10^6 enhanced green fluorescent protein mesenchymal stem cells (EGFP-MSCs). The unilateral 6-OHDA lesion was performed on day 0, EGFP-MSCs (5×10^5) were applied intranasally on days 7 and 9. (**A**) Stepping test results shown as the ratio between contralateral (Parkinsonian) forepaw stepping and ipsilateral forepaw stepping ($^*p<0.05$, $^{**}p<0.01$; cell-treated vs. control group on respective test days using Fisher least significant difference [LSD] *post hoc* test; $n=9$ cell-treated vs. $n=7$ control animals). (**B**) D-amphetamine (2 mg/kg)-induced net ipsilateral rotations (ipsilateral minus contralateral) between 30 and 120 min postinjection ($^*p<0.05$; cell-treated vs. control tested for each day using a one-way analysis of variance [ANOVA]; $n=12$ cell-treated vs. $n=10$ control). Data are presented as mean ± standard error of the mean (SEM).

neuronal BDNF level *in vitro*.[39] Moreover, here we show that the levels of IL-1β, IL-2, -6, -12, TNF-α, IFN-γ, and GM-CSF were dramatically increased in the lesioned brain halves of control groups 4.5 months after the 6-OHDA lesion. Among the inflammatory cytokines, TNF-α, IL-1β, IL-2, and IL-6 appear to be prominently upregulated in striatum and SN of PD patients and in the brains of animals affected by AD-like pathology.[32,40,41] TNF-α and IFN-γ are known to regulate the migration of MSCs[42] and may be also responsible for the targeted migration of INA MSCs shown here. Thus, it is likely that not only in PD, but also in AD, IN administration of MSCs would lead to targeted migration of these cells to the areas burdened by specific neurodegenerative changes like Abeta plaque deposition and inflammation. MSCs are capable of differentiating to a cholinergic neuron-like phenotype, to metabolize Abeta, to decrease the Abeta-induced inflammatory response in neural cells,[43] and to improve the cognitive impairment in AD mice after surgical transplantation.[44] Therefore, noninvasive IN delivery of MSCs into brains affected by AD pathology may further improve the therapeutic effects of these cells by increasing their survival and migration toward the areas affected by Abeta plaques and inflammation. The strong antiinflammatory activity of MSCs, reflected by their capacity to decrease the levels of IL-1β, IL-2, -6, -12, TNF-α, IFN-γ, and GM-CSF in the lesioned brain, provides further evidence for their role as powerful modulators of the immune response as described in the literature: MSCs suppress activation of natural killer cells and T cells.[45,46]

The comparison of results from two different behavioral tests shows that INA of MSCs significantly, but weakly, compensated the 6-OHDA–induced dysbalance between the hemispheres (resulting in rotational behavior) whereas motor control of the forepaws (the stepping test) was prominently improved. This discrepancy could be explained by a better restoration of dopaminergic activity in the SN than in the striatum. Indeed the recovery of TH expression in the SN of the cell-treated group is more prominent than in the striatum when compared with the respective ipsilateral structure of the control group (Fig. 2). This is strongly supported by recent findings of Mukhida et al.,[47] suggesting that the reinnervation of the striatum appears to be important for restoration of rotational symmetry, whereas reinnervation of the SN and/or the subthalamic nucleus may be necessary for more complex sensorimotor behaviors reflected by the stepping test without restoration of rotational symmetry.[48] Because basal ganglia dopamine preferentially controls fine movement of the forepaws and face in quadrupeds,[49] testing of fine motor control of the forepaws (the stepping test) correlates better with the human condition of sensorimotor deficits related to Parkinsonism than rotational behavior.[47]

Our data suggest that despite their ability to express TH, it is likely that INA MSCs function more in a neuroprotective and antiinflammatory manner rather than by replacing degenerated dopaminergic neurons. Recently, beneficial effects of INA of MSCs were shown in an animal model of neonatal ischemic brain damage.[50] Therefore, IN delivery of therapeutic cells to the CNS can serve as a noninvasive alternative to the current traumatic surgical procedure of transplantation. Moreover chronic treatment using the IN delivery method will increase the number of delivered cells to the brain and thus would likely enhance the therapeutic benefit. IN application of MSCs is worthy of further testing as a treatment for PD.

Acknowledgments

The authors wish to thank Sonja Seeger-Armbruster, Nadine Lettfuss, and Carina Stegmayr for excellent assistance during surgery and cell application.

AuthorDisclosure Statement

No competing financial interests exist.

References

1. Kozlowska H, Jablonka J, Janowski M, Jurga M, Kossut M, Domanska-Janik K. Transplantation of a novel human cord blood-derived neural-like stem cell line in a rat model of cortical infarct. Stem Cells Dev 2007;16:481–488.
2. Sinden, JD, Patel SN, Hodges H. Neural transplantation: Problems and prospects for therapeutic application. Curr Opin Neurol Neurosurg 1992;5:902–908.
3. Perry V, Andersson P, Gordon S. Macrophages and inflammation in the central nervous system. Trends Neurosci 1993;16:268–273.
4. Finsen B, Sorensen T, Castellano B, Pedersen E, Zimmer J. Leukocyte infiltration and glial reactions in xenografts of mouse brain tissue undergoing rejection in the adult rat brain: A light and electron microscopical immunocytochemical study. J Neuroimmunol 1991;32:159–183.
5. McKeon R, Schreiber R, Rudge J, Silver J. Reduction of neurite outgrowth in a model of glial scarring following CNS injury is correlated with the expression of inhibitory molecules on reactive astrocytes. J Neurosci 1991;11:3398–3411.
6. Barker RA, Dunnett SB, Faissner A, Fawcett JW. The time course of loss of dopaminergic neurons and the gliotic reaction surrounding grafts of embryonic mesencephalon to the striatum. Exp Neurol 1996;141:79–93.
7. Coyne TM, Marcus AJ, Reynolds K, Black IB, Woodbury D. Disparate host response and donor survival after the transplantation of mesenchymal or neuroectodermal cells to the intact rodent brain. Transplantation 2007;84:1507–1516.
8. Coyne TM, Marcus AJ, Woodbury D, Black IB. Marrow stromal cells transplanted to the adult brain are rejected by an inflammatory response and transfer donor labels to host neurons and glia. Stem Cells 2006;24:2483–2492.
9. Kraitchman DL, Tatsumi M, Gilson WD, Ishimori T, Kedziorek D, Walczak P, Segars WP, Chen HH, Fritzges D, Izbudak I, Young RG, Marcelino M, Pittengert MF, Solaiyappan M, Boston RC, Tsui BMW. Dynamic imaging of allogeneic mesenchymal stem cells trafficking to myocardial infarction. Circulation 2005;112:1451–1461.
10. Hauger O, Frost EE, van Heeswijk R, Deminiere C, Xue R, Delmas Y, Combe C, Moonen CTW, Grenier N, Bulte JWM. MR evaluation of the glomerular homing of magnetically labeled mesenchymal stem cells in a rat model of nephropathy. Radiology 2006;238:200–210.
11. Walczak P, Zhang J, Gilad AA, Kedziorek DA, Ruiz-Cabello J, Young RG, Pittenger MF, van Zijl PC, Huang J, Bulte JW. Dual-modality monitoring of targeted intraarterial delivery of mesenchymal stem cells after transient ischemia. Stroke 2008;39:1569–1574.
12. Olsen TS, Bruhn P, Oberg RG. Cortical hypoperfusion as a possible cause of 'subcortical aphasia'. Brain 1986;109:393–410.
13. Ceravolo R, Volterrani D, Gambaccini G, Rossi C, Logi C, Manca G, Berti C, Mariani G, Murri L, Bonuccelli U. Dopaminergic degeneration and perfusional impairment in Lewy body dementia and Alzheimer's disease. Neurol Sci 2003; 24:162–163.
14. Kikuchi A, Takeda A, Kimpara T, Nakagawa M, Kawashima R, Sugiura M, Kinomura S, Fukuda H, Chida K, Okita N, Takase S, Itoyama Y. Hypoperfusion in the supplementary motor area, dorsolateral prefrontal cortex and insular cortex in Parkinson's disease. J Neurol Sci 2001;193:29–36.
15. Danielyan L, Schafer R, von Ameln-Mayerhofer A, Buadze M, Geisler J, Klopfer T, Burkhardt U, Proksch B, Verleysdonk S, Ayturan M, Nuniatian GH, Gleiter CH, Frey WH 2nd. Intranasal delivery of cells to the brain. Eur J Cell Biol 2009;88:315–324.
16. van den Brandt J, Wang D, Kwon SH, Heinkelein M, Reichardt HM. Lentivirally generated eGFP-transgenic rats allow efficient cell tracking in vivo. Genesis 2004;39:94–109.
17. Ji JF, He BP, Dheen ST, Tay SS. Interactions of chemokines and chemokine receptors mediate the migration of mesenchymal stem cells to the impaired site in the brain after hypoglossal nerve injury. Stem Cells 2004;22:415–427.
18. Paxinos G, Watson C (eds.). The rat brain in stereotaxic coordinates. Academic Press, San Diego, 1996.
19. Heffner TG, Hartman JA, Seiden LS. A rapid method for the regional dissection of the rat brain, Pharmacol Biochem Behav 1980;13:453–456.
20. Mayerhofer A, Kovar K-A, Schmidt WJ. Changes in serotonin, dopamine and noradrenaline levels in striatum and nucleus accumbens after repeated administration of the abused drug MDMA in rats. Neurosci Lett 2001;13:453–456.
21. Olsson M, Nikkhah G, Bentlage C, Björklund A. Forelimb akinesia in the rat Parkinson model: differential effects of dopamine agonists and nigral transplants as assessed by a new stepping test. J Neurosci 1995;15:3863–3875.
22. Tillerson JL, Cohen AD, Philhower J, Miller GW, Zigmond MJ, Schallert T. Forced limb-use effects on the behavioral and neurochemical effects of 6-hydroxydopamine. J Neurosci 2001;21:4427–4435.
23. Anagnostaras SG, Robinson TE. Sensitization to the psychomotor stimulant effects of amphetamine: modulation by associative learning. Behav Neurosci 1996;110:1397–1414.
24. Schmidt WJ, Tzschentke TM, Kretschmer BD. State-dependent blockade of haloperidol induced sensitisation of catalepsy by MK-801. Eur J Neurosci 1999;11:3365–3368.
25. Banjaw MY, Mayerhofer A, Schmidt WJ. Anticataleptic activity of cathinone and MDMA (Ecstasy) upon acute and subchronic administration in rat. Synapse 2003;49:232–238.
26. Schmidt WJ, Lebsanft H, Heindl M, Gerlach M, Gruenblatt E, Riederer P, Mayerhofer A, Scheller DKA. Continuous versus pulsatile administration of rotigotine in 6-OHDA-lesioned rats: contralateral rotations and abnormal involuntary movements. J Neural Transm 2008;115:1385–1392.
27. Bradford MM. A rapid and sensitive method for the quantitation of microgram quantities of protein utilizing the principle of protein-dye binding. Anal Biochem 1976;72:248–254.
28. Danielyan L, Lourhmati A, Verleysdonk S, Kabisch D, Proksch B, Thiess U, Umbreen S, Schmidt B, Gleiter CH. Angiotensin receptor type 1 blockade in astroglia decreases hypoxia-induced cell damage and TNF alpha release. Neurochem Res 2007;32:1489–1498.
29. Trzaska KA, King CC, Li KY, Kuzhikandathil EV, Nowycky MC, Ye JH, Rameshwar P. Brain-derived neurotrophic factor facilitates maturation of mesenchymal stem cell-derived dopamine progenitors to functional neurons. J Neurochem 2009;110:1058–1069.
30. Binger T, Stich S, Andreas K, Kaps C, Sezer O, Notter M, Sittinger M, Ringe J. Migration potential and gene expression profile of human MSC induced by CCL25. Exp Cell Res 2009;315:1468–1479.
31. Seeger-Armbruster and von Ameln-Mayerhofer, unpublished results.
32. Hirsch EC, Hunot S. Neuroinflammation in Parkinson's disease: A target for neuroprotection? Lancet Neurol 2009;8: 382–397.

33. Ungerstedt U, Arbuthnott GW. Quantitative recording of rotational behavior in rats after 6-hydroxy-dopamine lesions of the nigrostriatal dopamine system. Brain Res 1970;24:485–493.
34. Thorne RG, Pronk GJ, Padmanabhan V, Frey WH. Delivery of insulin-like growth factor-I to the rat brain and spinal cord along olfactory and trigeminal pathways following intranasal administration. Neuroscience 2004;127:481–496.
35. Dhuria, SV, Hanson, LR and Frey, WH II. Intranasal delivery to the central nervous system: mechanisms and experimental considerations. J Pharmaceut Sci 2010;99:1654–1673.
36. Bäckman CM, Shan L, Zhang YJ, Hoffer BJ, Leonard S, Troncoso JC, Vonsatel P, Tomac AC. Gene expression patterns for GDNF and its receptors in the human putamen affected by Parkinson's disease: A real-time PCR study. Mol Cell Endocrinol 2006;252:160–166.
37. Nagatsu T, Mogi M, Ichinose H, Togari A. Cytokines in Parkinson's disease. J Neural Transm Suppl 2000;58:143–151.
38. Angelucci F, Spalletta G, di Iulio F, Ciaramella A, Salani F, Colantoni L, Varsi AE, Gianni W, Sancesario G, Caltagirone C, Bossu P. Alzheimer's disease (AD) and mild cognitive impairment (MCI) patients are characterized by increased BDNF serum levels. Curr Alzheimer Res 2010;7:15–20.
39. Aliaga E, Silhol M, Bonneau N, Maurice T, Arancibia S, Tapia-Arancibia L. Dual response of BDNF to sublethal concentrations of beta-amyloid peptides in cultured cortical neurons. Neurobiol Dis 2010;37:208–217.
40. Patel NS, Paris D, Mathura V, Quadros AN, Crawford FC, Mullan MJ. Inflammatory cytokine levels correlate with amyloid load in transgenic mouse models of Alzheimer's disease. J Neuroinflammation 2005;2:9.
41. Danielyan L, Klein R, Hanson LR, Buadze M, Schwab M, Gleiter CH, Frey WH. Protective effects of intranasal losartan in the APP/PS1 transgenic mouse model of Alzheimer disease. Rejuvenation Res 2010;13:195–201.
42. Hemeda H, Jakob M, Ludwig A, Giebel B, Lang S, Brandau S. Interferon-gamma and tumor necrosis factor-alpha differentially affect cytokine expression and migration properties of mesenchymal stem cells. Stem Cells Dev 2010;19: 693–706.
43. Danielyan L, Schafer R, Schulz A, Ladewig T, Lourhmati A, Buadze M, Schmitt AL, Verleysdonk S, Kabisch D, Koeppen K, Siegel G, Proksch B, Kluba T, Eckert A, Kohle C, Schoneberg T, Northoff H, Schwab M, Gleiter CH. Survival, neuron-like differentiation and functionality of mesenchymal stem cells in neurotoxic environment: the critical role of erythropoietin. Cell Death Differ 2009;16:1599–1614.
44. Lee JK, Jin HK, Endo S, Schuchman EH, Carter JE, Bae JS. Intracerebral transplantation of bone marrow-derived mesenchymal stem cells reduces amyloid-beta deposition and rescues memory deficits in Alzheimer's disease mice by modulation of immune responses. Stem Cells 2010;28:329–343.
45. Krampera M, Glennie S, Dyson J, Scott D, Laylor R, Simpson E, Dazzi F. Bone marrow mesenchymal stem cells inhibit the response of naive and memory antigen-specific T cells to their cognate peptide. Blood 2003;101:3722–3729.
46. Sotiropoulou PA, Perez SA, Gritzapis AD, Baxevanis CN, Papamichail M Interactions between human mesenchymal stem cells and natural killer cells. Stem Cells 2006;24:74–85.
47. Mukhida K, Baker KA, Sadi D, Mendez I. Enhancement of sensorimotor behavioral recovery in hemiparkinsonian rats with intrastriatal, intranigral, and intrasubthalamic nucleus dopaminergic transplants. J Neurosci 2001;21:3521–3530.
48. Nikkhah G, Cunningham MG, Jödicke A, Knappe U, Björklund A. Improved graft survival and striatal reinnervation by microtransplantation of fetal nigral cell suspensions in the rat Parkinson model. Brain Res 1994;633:133–143.
49. Meredith GE, Kang UJ. Behavioral models of Parkinson's disease in rodents: A new look at an old problem. Mov Disord 2006;21:1595–1606.
50. van Velthoven CT, Kavelaars A, van Bel F, Heijnen CJ. Nasal administration of stem cells: a promising novel route to treat neonatal ischemic brain damage. Pediatr Res 2010;68:419–422.

Address correspondence to:
Lusine Danielyan, M.D.
Department of Clinical Pharmacology
University Hospital of Tuebingen
Otfried-Mueller Str. 45
D-72076 Tübingen
Germany

E-mail: lusine.danielyan@med.uni-tuebingen.de

Received: November 2, 2010
Accepted: November 20, 2010

This article has been cited by:

1. Margaret S Landis, Tracey Boyden, Simon Pegg. 2012. Nasal-to-CNS drug delivery: where are we now and where are we heading? An industrial perspective. *Therapeutic Delivery* **3**:2, 195-208. [CrossRef]
2. Dan B. Renner, William H. Frey Ii, Leah R. Hanson. 2012. Intranasal Delivery of siRNA to the Olfactory Bulbs of Mice via the Olfactory Nerve Pathway. *Neuroscience Letters* . [CrossRef]
3. Alexander Storch, Ilona Csoti, Karla Eggert, Tove Henriksen, Annika Plate, Michael Lorrain, Wolfgang H. Oertel, Angelo Antonini. 2012. Intrathecal application of autologous bone marrow cell preparations in parkinsonian syndromes. *Movement Disorders* n/a-n/a. [CrossRef]
4. Lidia Cova, Patrizia Bossolasco, Marie-Therese Armentero, Valentina Diana, Eleonora Zennaro, Manuela Mellone, Cinzia Calzarossa, Silvia Cerri, Giorgio Lambertenghi Deliliers, Elio Polli, Fabio Blandini, Vincenzo Silani. 2011. Neuroprotective effects of human mesenchymal stem cells on neural cultures exposed to 6-hydroxydopamine: implications for reparative therapy in Parkinson's disease. *Apoptosis* . [CrossRef]
5. Xinfeng Liu. 2011. Clinical trials of intranasal delivery for treating neurological disorders – a critical review. *Expert Opinion on Drug Delivery* **8**:12, 1681-1690. [CrossRef]
6. Jeffrey J. Lochhead, Robert G. Thorne. 2011. Intranasal Delivery of Biologics to the Central Nervous System. *Advanced Drug Delivery Reviews* . [CrossRef]
7. Y. Jiang, N. Wei, J. Zhu, D. Zhai, L. Wu, M. Chen, G. Xu, X. Liu. 2011. A new approach with less damage: intranasal delivery of tetracycline-inducible replication-defective herpes simplex virus type-1 vector to brain. *Neuroscience* . [CrossRef]
8. Gaia Colombo, Luca Lorenzini, Elisa Zironi, Viola Galligioni, Fabio Sonvico, Anna Giulia Balducci, Giampiero Pagliuca, Alessandro Giuliani, Laura Calzà, Alessandra Scagliarini. 2011. Brain distribution of ribavirin after intranasal administration. *Antiviral Research* . [CrossRef]
9. Stephen B. Dunnett, Anne E. Rosser. 2011. Clinical translation of cell transplantation in the brain. *Current Opinion in Organ Transplantation* 1. [CrossRef]
10. Yongjun Jiang, Juehua Zhu, Gelin Xu, Xinfeng Liu. 2011. Intranasal delivery of stem cells to the brain. *Expert Opinion on Drug Delivery* **8**:5, 623-632. [CrossRef]
11. Elena H. Chartoff, Diane Damez-Werno, Kai C. Sonntag, Linda Hassinger, Daniel E. Kaufmann, Jesse Peterson, Donna McPhie, Anne M. Cataldo, Bruce M. Cohen. 2011. Detection of Intranasally Delivered Bone Marrow-Derived Mesenchymal Stromal Cells in the Lesioned Mouse Brain: A Cautionary Report. *Stem Cells International* **2011**, 1-12. [CrossRef]